ELSEVIER

Journal of Chromatography A, 877 (2000) 225–232

JOURNAL OF CHROMATOGRAPHY A

www.elsevier.com/locate/chroma

Influence of ring opening–closure equilibrium of oxanine, a novel damaged nucleobase, on migration behavior in capillary electrophoresis

Toshinori Suzuki[a], Masaki Yamada[a], Hiroshi Ide[b], Kenji Kanaori[c], Kunihiko Tajima[c], Takashi Morii[a], Keisuke Makino[a,*]

[a]*Institute of Advanced Energy, Kyoto University, Gokasho, Uji 611-0011, Japan*

[b]*Department of Mathematical and Life Sciences, Graduate School of Science, Hiroshima University, Kagamiyama, Higashi-Hiroshima 739-8526, Japan*

[c]*Department of Polymer Science and Engineering, Kyoto Institute of Technology, Matsugasaki, Sakyo-ku, Kyoto 606-8585, Japan*

Received 13 December 1999; accepted 3 February 2000

Abstract

Oxanine (Oxa) is a novel damaged nucleobase which is generated from guanine by HNO_2 or NO. As a fundamental study for detection of Oxa formed in vivo, capillary zone electrophoresis (CZE) and micellar electrokinetic chromatography (MEKC) have been tested by changing the pH of the running buffer. At pH 7, CZE did not separate Oxa from seven other nucleobases, and MEKC separated Oxa but their peaks migrated close together. In both the techniques, an extreme peak broadening occurred for Oxa around pH 9 and a good peak separation was achieved at pH 12. The behavior of the Oxa peak is discussed in relation to the unique multistep acid–base equilibria of Oxa.

Keywords: Peak broadening; Ring opening–closure equilibrium; Oxanine; Nucleobase; Antibiotics

1. Introduction

Oxanosine (Oxo) [5-amino-3-β-(D-ribofuranosyl)-3H-imidazo-[4,5-d][1,3]oxazin-7-one], a ribonucleoside counterpart of oxanine (Oxa) (Fig. 1), was isolated for the first time as a novel antibiotic in 1981 from the culture broth of *Streptomyces capreolus* MG265-CF3 [1,2]. Oxa exhibited wide-range biological effects including antibacterial activity against *E. coli* K-12 and *Proteus mirabilis* IFM OM-9 [1] and reversion toward the normal phenotype of K-ras-transformed rat kidney cells [3].

Recently we have shown that the reaction of

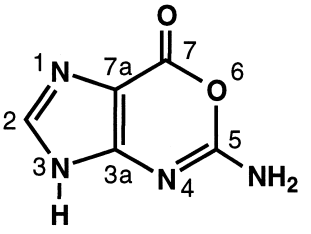

Fig. 1. Structure of oxanine (Oxa) with the atomic numbering.

*Corresponding author. Tel: +81-774-38-3517; fax: +81-774-38-3524.

E-mail address: kmak@iae.kyoto-u.ac.jp (K. Makino)

0021-9673/00/$ – see front matter
PII: S0021-9673(00)00178-3

2′-deoxyguanosine (dGuo) with nitrous acid (HNO_2) as well as with nitric oxide (NO) results in the formation of 2′-deoxyoxanosine (dOxo), a 2′-deoxyriboside counterpart of Oxa, and 2′-deoxyxanthosine (dXao), a deaminated product of dGuo [4], and that dOxo is also formed in a single-stranded oligodeoxynucleotide and double-stranded calf thymus DNA by HNO_2 treatment. Also, it has been demonstrated that *N*-nitrosoindoles, which can be formed from indoles in foodstuffs by endogenous nitrosation in the stomach, indirectly generate dOxo from dGuo at physiological pH via efficient nitroso group transfer to dGuo [5]. Regarding this unique product, it has been demonstrated that the *N*-glycosidic bond of dOxo is as stable as that of dGuo [6], and that 2′-deoxyoxanosine 5′-triphosphate is incorporated opposite thymine (Thy) as well as cytosine (Cyt) in the DNA template during DNA replication [7]. These results imply that the Oxa moiety generated from the guanine (Gua) moiety in the nucleotide pool or DNA may have an important role in mutagenic events in cells. However, though essentially necessary, there is no information on in vivo formation of Oxa so far. To assess the contribution of Oxa to HNO_2- and NO-induced cytotoxicity and genotoxicity, we need detection and quantitation methods for Oxa produced in DNA samples, urine, blood, and so on. Since these samples contain concomitant compounds, the essential requirement is to separate Oxa from them. We have already ruled out HPLC separation because of unsatisfactory resolution. One of the potent substitutions will be capillary electrophoresis (CE) which has extremely high resolution [8,9]. Another advantage of CE is that it is usable in wide pH range. This will be advantageous because Oxa, an *O*-acylisourea, changes its structure as well as its total charge through an ring opening–closure equilibrium under alkaline conditions [10]. Thus, the running buffer pH will be able to give a large influence to the migration of Oxa in CE.

We report herein the effect of the running buffer pH in the range of 7–12 on the migration of Oxa in the mixture with other seven nucleobases in capillary zone electrophoresis (CZE) and micellar electrokinetic chromatography (MEKC) [11,12]. We also discuss the migration behavior of Oxa in relation to spectrophotometric titration for acid–base equilibria of Oxa.

2. Experimental

2.1. Chemicals

2′-Deoxyguanosine (dGuo) was obtained from Yamasa, and xanthine (Xan), hypoxanthine (Hyp), guanine (Gua), uracil (Ura), adenine (Ade), thymine (Thy), and cytosine (Cyt) were from Wako. All other chemicals of reagent grade were purchased from Nacalai Tesque or Wako. All the reagents were used without further purification. Water was purified with a Millipore Milli-QII deionizer.

2.2. Apparatus

A capillary electrophoresis system consisted of an AMS (Advanced Molecular Science) model 2000 interfaced with a data processing computer. Electrophoretic separation was performed using a fused-silica tubing (700 mm×75 μm I.D.) which was thermostated at 30°C by a liquid thermal control system. The effective column length to the UV absorbance detector was 650 mm. A sample (10 nl) was injected into the capillary tube by pressure. UV absorbance was recorded by the on-column detection at 247, 263, and 287 nm simultaneously. The buffer used for CZE was 10 m*M* NaH_2PO_4–$Na_2B_4O_7$ (pH 7–9) and 10 m*M* $Na_2B_4O_7$–NaOH (pH 10–12). The same buffer containing 75 m*M* sodium dodecyl sulfate (SDS) was used for MEKC. The applied voltage and current were as follows: 12.0 kV, 7.1 μA (pH 7), 12.4 kV, 8.0 μA (pH 8), 12.2 kV, 8.9 μA (pH 9), 12.4 kV, 9.4 μA (pH 10), 11.7 kV, 9.7 μA (pH 11), 12.7 kV, 12.1 μA (pH 12) for CZE and 11.2 kV, 19.6 μA (pH 7), 11.2 kV, 20.7 μA (pH 8), 11.2 kV, 21.1 μA (pH 9), 11.7 kV, 22.9 μA (pH 10), 11.9 kV, 24.9 μA (pH 11), 12.8 kV, 27.3 μA (pH 12) for MEKC.

2.3. Preparation of Oxa

2′-Deoxyoxanosine (dOxo) was obtained by nitrous acid treatment of dGuo and subsequent reversed-phase (RP) HPLC separation as described previously [6]. To obtain Oxa from dOxo, 10 m*M* dOxo was incubated in 1 *M* HCl at 37°C for 2 h. Oxa was separated from the reaction mixture by RP-HPLC with 100 m*M* triethylammonium acetate buffer (pH 7) containing acetonitrile, subsequently

desalted by RP-HPLC employing an eluent of acetonitrile–water, and finally lyophilized.

2.4. Spectrophotometric pH titration of Oxa

pH-titrated UV spectra were obtained on a Beckman DU-68 spectrometer at room temperature. Oxa (30 μM) was dissolved in 10 ml of water, and the pH was adjusted by conc. HCl or NaOH.

2.5. Calculations

The number of theoretical plates (N) was calculated by the following equation:

$$N = 5.54 \left(\frac{t}{w_{1/2}} \right)^2$$

where t is the migration time (s) and $w_{1/2}$ is the width (in time units) at 50% maximum peak height.

The electrophoretic mobility (μ_{ep}) was calculated using the following equation:

$$\mu_{ep} = lL/t_0V - lL/tV \ (\mathrm{cm^2\ V^{-1}\ s^{-1}})$$

where l and L are the length of the capillary to the detector and the total length of the capillary, respectively. V is the applied potential. The terms t and t_0 are the migration times of anions and a neutral marker, respectively.

3. Results and discussion

3.1. pH dependent separation in CZE

The pH dependence of separation of the mixture of Oxa and seven nucleobases (Xan, Hyp, Gua, Ura, Ade, Thy, and Cyt) was examined using CZE in the pH range of running buffer from 7 to 12. The peaks of the nucleobases in the mixed sample were assigned on the basis of the agreement of the capillary electrophoresis (CE) migration time and/or the ratio of UV absorbance at 245, 263, and 287 nm of individually injected authentic samples. The sample

Table 1
Molecular mass (M_r), pK_a values, and solubility (g/100 ml water) of nucleobases[a]

Compound	M_r	pK_{a1}	pK_{a2}	Solubility
Oxa	152	9.4[b]	8.5[b]	–
Xan	152	7.4	11.1	0.05(20°C)
Hyp	136	8.9	12.1	0.07(15°C)
Gua	151	9.2	12	0.004(40°C)
Ura	112	9.5	>13	0.36(25°C)
Ade	135	9.8	–	0.09(25°C)
Thy	126	9.9	>13	0.4(25°C)
Cyt	111	12.2	–	0.77(25°C)

[a] From Ref. [13].
[b] Present work.

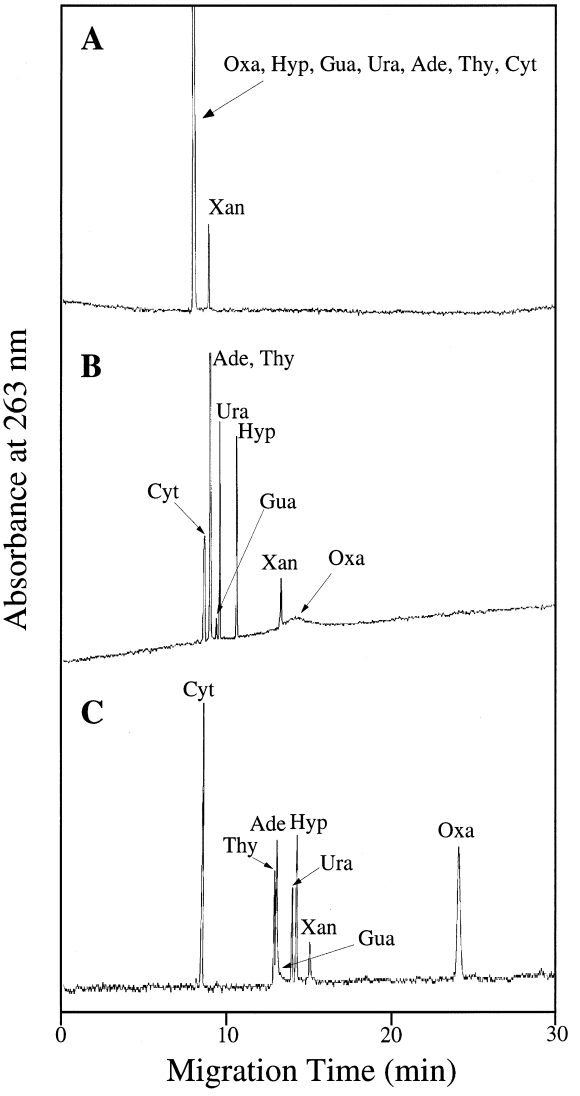

Fig. 2. Electropherogram obtained for nucleobases (Oxa, Xan, Hyp, Gua, Ura, Ade, Thy, and Cyt) by CZE mode. The separation was carried out at (A) pH 7.0 and (B) pH 9.0 in 10 mM NaH_2PO_4–$Na_2B_4O_7$ buffer and at (C) pH 12.0 in 10 mM $Na_2B_4O_7$–NaOH buffer.

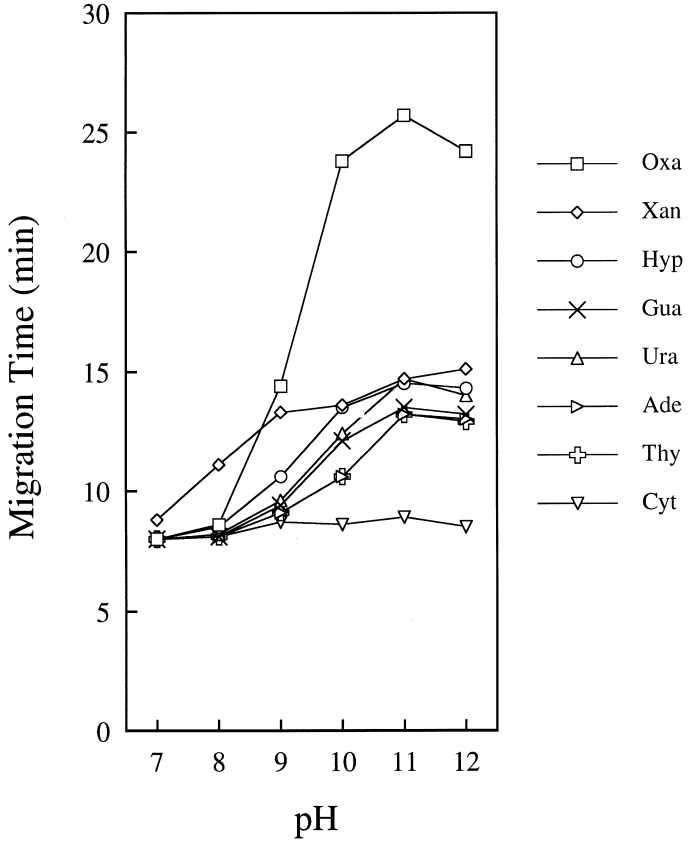

Fig. 3. Effect of electrolyte pH on nucleobases separation by CZE.

concentration of the nucleobases was 100 μ*M* except Gua for which a solution saturated at room temperature was used. The pK_a values and the water solubility of the nucleobases [13] are summarized in Table 1 together with those determined for Oxa in this work. Figs. 2A, 2B, and 2C show the electropherograms obtained for the mixed sample at pH 7, 9, and 12, respectively. Using the data in Fig. 2, the migration time of each nucleobase is plotted against the pH in Fig. 3. At pH 7, all the nucleobases

Table 2
pH dependence of the number of theoretical plates (*N*) in CZE separation

Compound	Number of theoretical plates (*N*)					
	pH 7	pH 8	pH 9	pH 10	pH 11	pH 12
Oxa	coel.[a]	coel.	200	9 000	47 800	73 000
Xan	101 000	108 800	226 500	coel.	coel.	73 000
Hyp	coel.	coel.	226 600	14 600	105 700	181 200
Gua	coel.	coel.	113 300	coel.	58 700	coel.
Ura	coel.	coel.	118 700	136 600	107 600	98 400
Ade	coel.	coel.	coel.	coel.	coel.	84 800
Thy	coel.	coel.	coel.	coel.	coel.	212 800
Cyt	coel.	coel.	24 100	23 600	31 400	64 800

[a] coel.: coeluting peaks

except Xan coeluted (Fig. 2A). It should be noted that seven species out of the eight nucleobases are uncharged at pH 7 and Xan has an acid–base equilibrium near pH 7 ($pK_a = 7.4$) (Table 1). CZE efficiently separates charged solutes based on their different electrophoretic mobility [8]. The considerably large migration time of Xan relative to other nucleobases is, therefore, attributed to the partial ionization of this solute to a negatively charged species.

The increase in pH of the buffer solution resulted in an increase in the migration time of all nucleobases except Cyt (Fig. 2B and 2C). At pH 9, the order of the migration time was Xan>Hyp>Ura>Gua>Ade=Thy (Fig. 2B). This order essentially correlated with that of the pK_{a1} values. Inversion of the order of the migration times and pK_{a1} values between Gua and Ura is probably due to the effect of the molecular size [8]. Over the pH range examined, the peak intensity of Gua was considerably small due to its extreme low solubility (Table 1). The largest increase in the migration time with increasing pH was observed for Oxa (Fig. 3). An extreme broadening of the Oxa peak occurred at pH 9 (Fig. 2B), while the peak broadening was not observed for the other nucleobases over the pH range examined (see Table 2). The number of theoretical plates (N) of Oxa was as low as 200 at pH 9. On the other hand, at pH 12, the Oxa peak was sharp (Fig. 2C) and completely separated from the other nucleobases.

3.2. pH dependent separation in MEKC

The effective separation of the four nucleobases (Ura, Ade, Thy, and Cyt) has been reported using micellar electrokinetic chromatography (MEKC) at neutral pH [12]. We examined this method for our sample in the pH range 7–12. Fig. 4A– C show the electropherograms of the nucleobases obtained by MEKC at pH 7, 9, and 12, respectively. Fig. 5 and Table 3 show the migration time and N of the nucleobase peaks, respectively. At pH 7, the nucleobases migrated in sharp peaks and Oxa was separated from the other nucleobases (Fig. 4A). However, all nucleobases migrated fast and their peaks stood close together. The increase in pH of buffer solution resulted in the increased migration time for all nucleobases except Cyt (Fig. 5). The

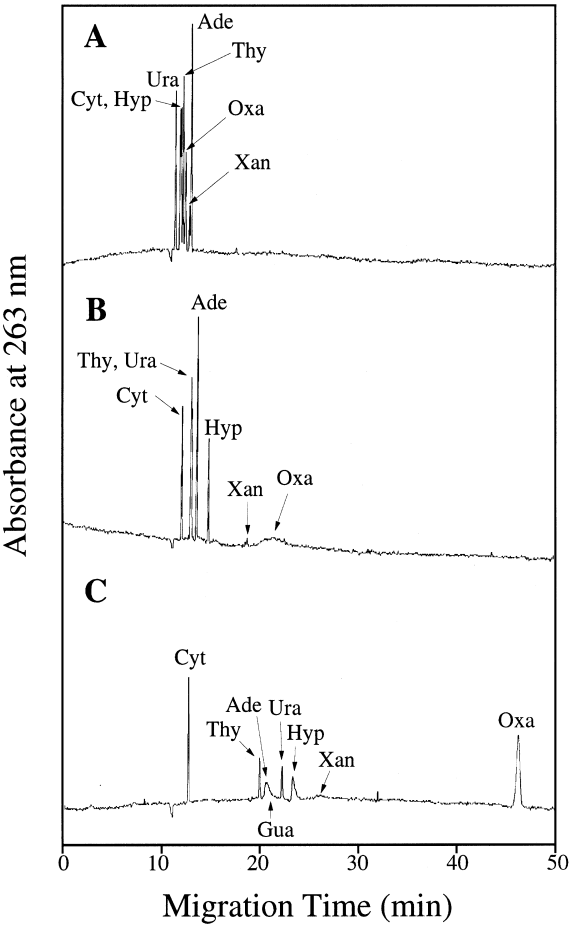

Fig. 4. Electropherogram obtained for nucleobases (Oxa, Xan, Hyp, Gua, Ura, Ade, Thy, and Cyt) by MEKC mode. The separation was carried out with 75 m*M* SDS at (A) pH 7.0 and (B) pH 9.0 in 10 m*M* NaH_2PO_4–$Na_2B_4O_7$ buffer, and at (C) pH 12.0 in 10 m*M* $Na_2B_4O_7$–NaOH buffer.

order of the migration time of nucleobases in MEKC was the same as that in CZE separation. The peak of Gua was weak and could not be detected at pH 7 and 9. The migration time of Oxa showed an large increase around pH 9 (Fig. 5). Extreme peak broadening ($N = 400$) occurred for Oxa at pH 9 (Fig. 4B and Table 3). At pH 12, the Oxa peak migrated more slowly, became sharp and was well separated from the other peaks (Fig. 4C). However, the peaks of Ade, Gua, Hyp, and Xan were broadened at pH 12 for unknown reasons. The optimal pH for the separation of Oxa by MEKC was 12.

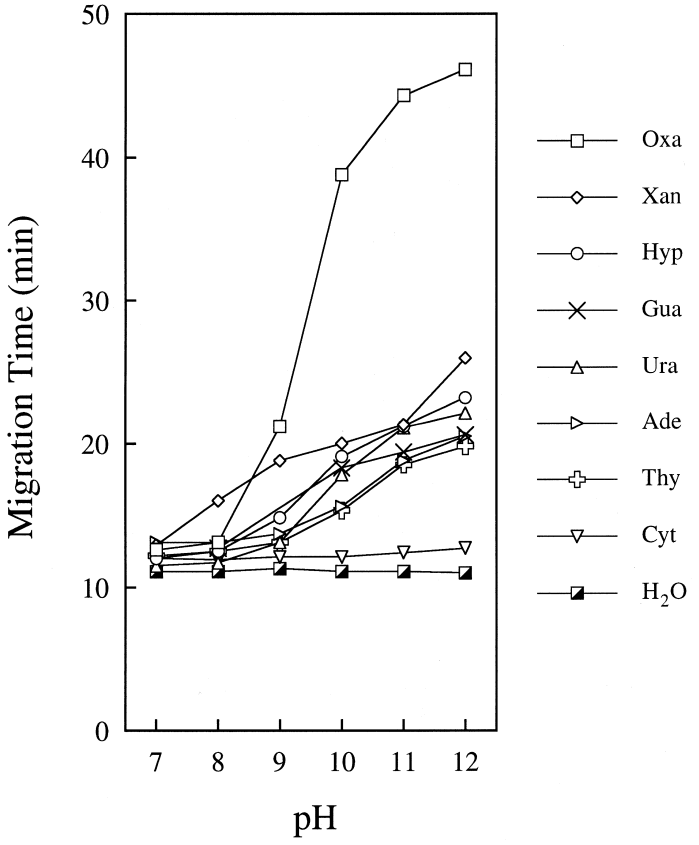

Fig. 5. Effect of electrolyte pH on nucleobases separation by MEKC.

3.3. Acid–base equilibria of Oxa

Oxa has a six membered ring, *O*-acylisourea. The acid–base equilibrium of *O*-acylisourea has been well investigated for an oxazine, 2-amino-4,5-benzo-6-oxo-1,3-oxazine [13]. By spectrophotometric titration and kinetic data, the presence of three species was established for the oxazine in the pH range

Table 3
pH dependence of the number of theoretical plates (*N*) in MEKC separation

Compound	Number of theoretical plates (*N*)					
	pH 7	pH 8	pH 9	pH 10	pH 11	pH 12
Oxa	50 900	coel.[a]	400	8 900	36 500	75 900
Xan	77 100	118 100	83 600	72 200	21 000	1 000
Hyp	coel.	coel.	70 700	66 300	coel.	27 800
Gua	n.d.[a]	74 500	n.d.	31 700	177 500	coel.
Ura	42 400	99 800	coel.	57 500	coel.	88 300
Ade	55 400	55 400	86 600	78 700	41 200	5 400
Thy	48 300	coel.	coel.	107 900	110 100	93 200
Cyt	coel.	45 700	47 400	67 500	71 000	51 800

[a] coel.: coeluting peaks; n.d.: not detected.

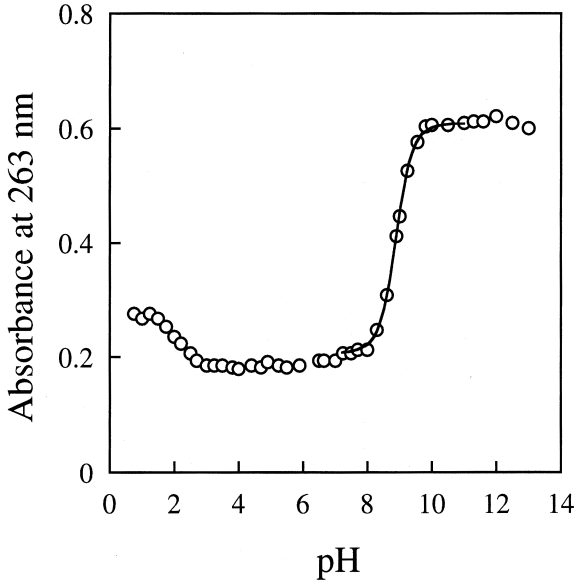

Fig. 6. pH-dependent change in the absorbance of Oxa at 263 nm. The solid line shows the theoretical curve obtained by the equation of Roth and Bunnett [14] (see text).

between 7 and 12. At pH 7, the oxazine exists as a ring-closed species with no charge. Oxazine loses a proton as increasing pH and undergoes the subsequent ring opening to yield a monovalent anion ($pK_{a1}=10.6$). A further increase in pH results in the loss of an additional proton to give rise to a divalent anion species ($pK_{a2}=9.2$). Owing to the unusual order of pK_a for oxazine ($pK_{a1}>pK_{a2}$), the monovalent anion is never present in greater than 10% mol fraction at any pH. In our previous work on dOxo, the presence of acid–base equilibria in the alkaline pH range was revealed by spectrophotometric titration [6]. The ring-opened species of dOxo was confirmed by ^{13}C-NMR measurement, which showed the resonance attributed to a carboxyl group. We have also shown that this equilibrium is a rather slow process relative to the NMR time scale, since ^{1}H-NMR signals attributable to both the ring-opened and -closed species were observed simultaneously.

In Fig. 6, the observed absorbances of Oxa at 263 nm are plotted against pH. Oxa showed a distinct change in absorbance around pH 9. The experimental data did not agree with the theoretical curve expected for a single monoionizable group (data not shown). Accordingly, a combination of two pK_as is expected to be involved in this pH region as in the case for the oxazine. The two pK_a values were determined by employing the equation of Roth and Bunnett [14]:

$$A_{aH} = (A_1 a_H^2 + A_3 K_{a1} a_H + A_2 K_{a1} K_{a2})/(a_H^2 + K_{a1} a_H + K_{a1} K_{a2})$$

where A_1 and A_3 are the absorption of the uncharged species and the ring-opened divalent anion species, respectively. A_2 is the absorption of the intermediate, i.e., the monovalent anion species. A_{a_H} is the observed absorption at a given proton concentration (a_H). The theoretical curve fitting for the experimental spectral data using this equation gave $pK_{a1}=9.4$, $pK_{a2}=8.5$, and $A_2=0.42$. The proposed acid–base equilibria for Oxa are shown in Fig. 7. While Oxa exists as the uncharged ring-closed form at neutral pH, the dominant species of Oxa is the ring-opened divalent anion form above pH 10. The fraction of the monovalent anion is expected low at any pH due to $pK_{a1}>pK_{a2}$.

The electrophoretic mobility (μ_{ep}) of Oxa at pH 11 in CZE was evaluated using Cyt as a neutral marker. The value of μ_{ep} ($4.85\cdot10^{-4}$ cm^2 V^{-1} s^{-1})

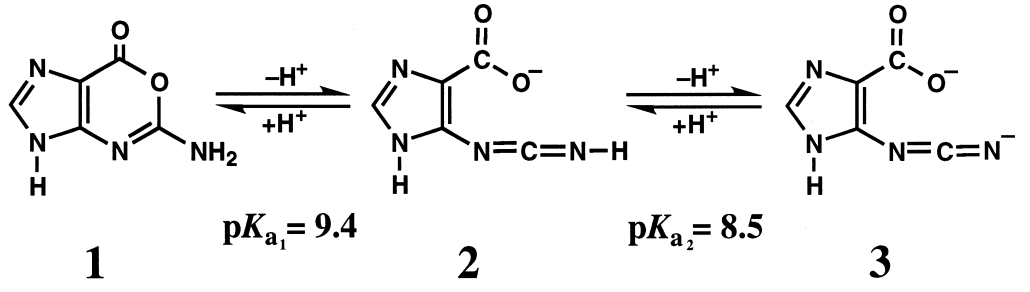

Fig. 7. Proposed acid–base equilibria of Oxa in the pH range 7–12.

was 1.9-fold greater than those for both Ade and Thy. At pH 11, the dominant species is the divalent anion for Oxa and monovalent anion for Ade and Thy according to their pK_a values. The μ_{ep} is directly proportional to the charge and inversely proportional to the radius of analytes [8]. The above result implies that the increase of the migration time of Oxa is originated by the increased charge and negligible contribution of the radius change of Oxa accompanied by ring opening.

Except for Oxa, no peak broadening was observed for all nucleobases treated in CZE even at the pH values near their pK_a values. All these equilibria were originated from the release of an imino proton and did not involve a basic skeletal change of the analyte structure. The process should be fast enough relative to the time scale of CE. On the other hand, Oxa showed the extreme broadening of the peak at pH 9. Around pH 9, two protons are released from the exocyclic amino group of Oxa (Fig. 7). The first step (1→2) involves a proton release and ring opening simultaneously, while the second step (2→3) only involves a proton release. The process of the first step would be slow enough to generate a vast distribution in the CE migration time.

4. Conclusions

A good separation of Oxa from the other nucleobases was achieved by increasing the pH of the running buffer, particularly at pH 12 in both CZE and MEKC. The large increase of the migration time and the extreme peak broadening observed around pH 9 for Oxa in both the techniques were due to the formation of the divalent anion of Oxa and to the slow ring opening–closure equilibrium, respectively.

Acknowledgements

This work was supported partly by Grants-in-Aid for Scientific Research from the Ministry of Education, Science and Culture, Japan [to K.M. (11101001, 10151219, and 10878092), K.K. (09780545), and H.I.].

References

[1] N. Shimada, N. Yagisawa, H. Naganawa, T. Takita, M. Hamada, T. Takeuchi, H. Umezawa, J. Antibiot. 34 (1981) 1216.
[2] H. Nakamura, N. Yagisawa, N. Shimada, T. Takita, H. Umezawa, Y. Iitaka, J. Antibiot. 34 (1981) 1219.
[3] O. Itoh, K. Kuroiwa, S. Atsumi, K. Umezawa, T. Takeuchi, M. Hori, Cancer Res. 49 (1989) 996.
[4] T. Suzuki, R. Yamaoka, M. Nishi, H. Ide, K. Makino, J. Am. Chem. Soc. 118 (1996) 2515.
[5] L.T. Lucas, D. Gatehouse, D.E.G. Shuker, J. Biol. Chem. 274 (1999) 18319.
[6] T. Suzuki, Y. Matsumura, H. Ide, K. Kanaori, K. Tajima, K. Makino, Biochemistry 36 (1997) 8013.
[7] T. Suzuki, M. Yoshida, M. Yamada, H. Ide, M. Kobayashi, K. Kanaori, K. Tajima, K. Makino, Biochemistry 37 (1998) 11592.
[8] S.M. Lunte, D.M. Randzik, in: S.M. Lunte, D.M. Radzik (Eds.), Pharmaceutical and Biomedical Applications of Capillary Electrophoresis, Pergamon, Oxford, 1996, p. 3.
[9] J.P. Foley, E.S. Ahuja, in: S.M. Lunte, D.M. Radzik (Eds.), Pharmaceutical and Biomedical Applications of Capillary Electrophoresis, Pergamon, Oxford, 1996, p. 81.
[10] A.F. Hegarty, T.C. Bruice, J. Am. Chem. Soc. 92 (1970) 6561.
[11] S. Terabe, K. Otsuka, K. Ichikawa, A. Tsutiya, T. Ando, Anal. Chem. 56 (1984) 111.
[12] A.S. Cohen, S. Terabe, J.A. Smith, B.L. Karger, Anal. Chem. 59 (1987) 1021.
[13] T.A. Brown (Ed.), Molecular Biology Labfax, BIOS Scientific Publishers, Oxford, 1991, p. 55.
[14] B. Roth, J.F. Bunnett, J. Am. Chem. Soc. 87 (1965) 334.